CHAPTER 6: SILOS - A CASE STUDY

Pietro Croce[1], Maria Luisa Beconcini[1], Martina Muzzi[1], Elisa Rosso[1]

[1]Department of Civil and Industrial Engineering – Structural Division – Univ. of Pisa, Italy

Summary

Silos are warehouses equipped for receiving and unloading incoherent materials, usually cereals. The shape is determined by their function, so they are generally composed by slender cylinders, adjacent to each other, and with the bottom provided with inclined surface and a central hole, aimed to unload materials on the trucks below.

In several European countries, mostly in the Mediterranean area, many of these buildings date from the post-war period, so that they need accurate studies in order to determine their reliability and, eventually, to design interventions for their rehabilitation.

In the present chapter the studies conducted on a r.c. silo in central Italy is presented; the properties of materials, the theoretic basis of design and the techniques typical of the time have been accurately retrieved and employed for assessing the actual state of the structure.

1 INTRODUCTION

The silos are particular constructions used to store loose materials and granular products, such as cereals, in large quantities; with both a function of storage in the industrial production cycle, and as warehouses regulating the disposal of substances. They usually are composed of adjacent elements, called cells, which have a cylindrical shape with flared bottom; the overall configuration is strictly related to the activities undertaken inside, which are usually highly automated.

In the past, they were built with masonry structure; later on, the introduction of modern materials, steel and reinforced concrete, contributed sensibly to the development of new structural and architectural typologies. Between the two world wars, there was a wide diffusion of reinforced concrete silos for storing and refining cereals, especially in Italy, Germany, France, Libya and France, and, later, in Spain.

At present, some of these buildings, particularly well conserved, may be considered as part of the industrial heritage, that is worth preserving because of their historical importance and because they often represent a sort of landmark in our territories.

In what follows, the case-study of a reinforced concrete silo, dating back about a century ago, is presented. As well as many other reinforced concrete structures built during the 20th century, it needs maintenance works, renovations and repair of damages caused by degradation or accidental events, in order to preserve its aspect and its structural reliability. Before proceeding at the design of the preservation works, specific studies must be performed in order to know the actual conformation of the structural elements. Since the materials and the basis of design for r.c. structures in use at the time of construction are quite different from those in use today, an accurate recognition of the geometry of structural elements is needed; afterwards, on the basis of the design approaches and the characteristics of the materials commonly used at the time, the reinforcing of the structural elements can be obtained through a simulated project. Afterwards the actual characteristics of the materials must be acquired, so that the effective safety level can be assessed and, if the case, specific preservation works designed, on the basis of codes and methods currently in use.

As recommended in [5], the study has been setup following the standardized procedure of the ISO 13822 [1], which is aimed to the evaluation of the actual reliability of a structure, through a preliminary assessment and, if necessary, a detailed assessment, organized in accordance with the step-by-step procedure outlined in the flow chart shown in figure 1.

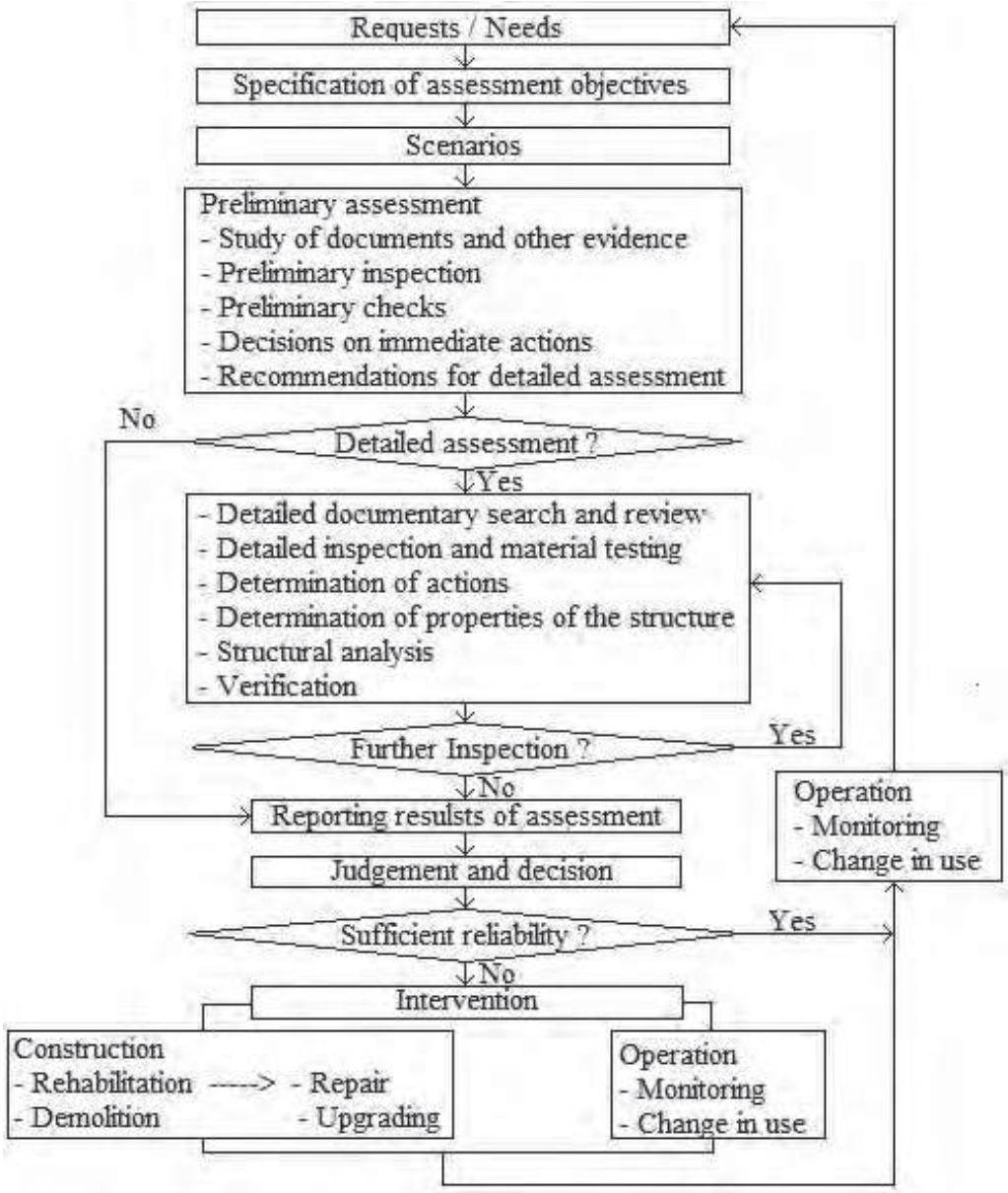

Figure 1 Flow chart of the ISO 13822

2 THE AGRICULTURAL CONSORTIUM SILO IN GROSSETO

The silo of the Agricultural Consortium of Grosseto (Tuscany, Italy) (figs. 2, 3), is one of the first reinforced concrete silos built in Tuscany (1933); it is still in use to amass and store cereals coming from the surroundings and from foreign countries, and it is considered a particular example of reinforced concrete monumental structures.

It is located near the town centre, just outside the ancient walls dating from the Medicean period and it was built very close to the railroad, so as to speed up the operations of loading and unloading, and it is part of a wider system of warehouses where goods were refined and then sold (figs. 4 and 5).

Figure 2 Main façade of the silo

Figure 3 Side view of the silo of the Agricultural Consortium of Grosseto

Figure 4 Localization of the silo

The silo was the first tall building of the town, with the essential and monumental shapes, typical of the rationalist and government architecture of the period. It was designed by the *Foundations and Construction Society* of Milan and was built, like many others in Italy and in the colonies, during the so called *wheat battle* promoted by the Italian fascist regime in the '30s, in order to control the price of cereals and to solve the food problem of the country.

Figure 5 Plan of the silo

3 PRELIMINARY ASSESSMENT

3.1 Study of the available documentation.

In the historical archive of Grosseto, only the original architectural design was found (fig. 6), which does not contain information about the structural configuration, the foundations, the properties of the materials, the quantity of reinforcing bars, and so on.

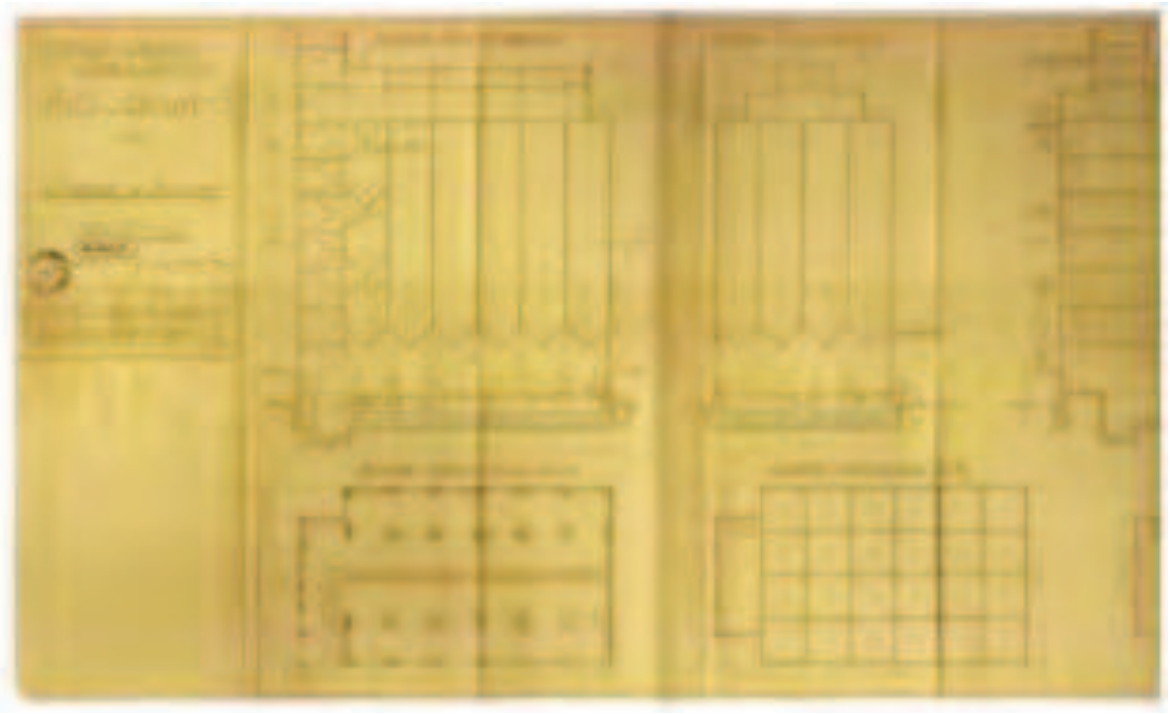

Figure 6 Original architectural drawings

Generally, silos have different dimensions, depending on the kind of goods stored, but the shape and the working principles are similar: usually, goods are put on horizontal conveyors at the ground floor and then sucked, by means of vertical conveyors to the top of the structure, in the so-called drying gallery; from here, cereals are deposited in the vertical cells.

As revealed by the architectural maps, the silo is divided in two different parts: the first one, bigger than the other, is composed of vertical cells, in which cereals are stored; the latter, called '*torretta*' (small tower), contains the staircase through which it is possible to go to the top of the building, to enter into the cells and the machinery for refining goods (figs. 7 and 8).

The first part of the silo consists of 32 vertical cells: twenty of them, adjacent to each other, are 3.80 × 3.80 × 18 m; the remaining twelve lay on three levels and are 3.80 × 3.80 × 6 m. At the ground floor there is the operating room, where are located the hoppers, truncated cone shaped. At the top of the building, there is the drying gallery.

The ground floor is characterized by a *pilotis* scheme, with rectangular columns. The cross section of the central columns is larger than that of external and corner ones, according to simplified design principles, mainly governed by compression stresses. The rectangular cells are composed by reinforced concrete walls, 17 cm thick.

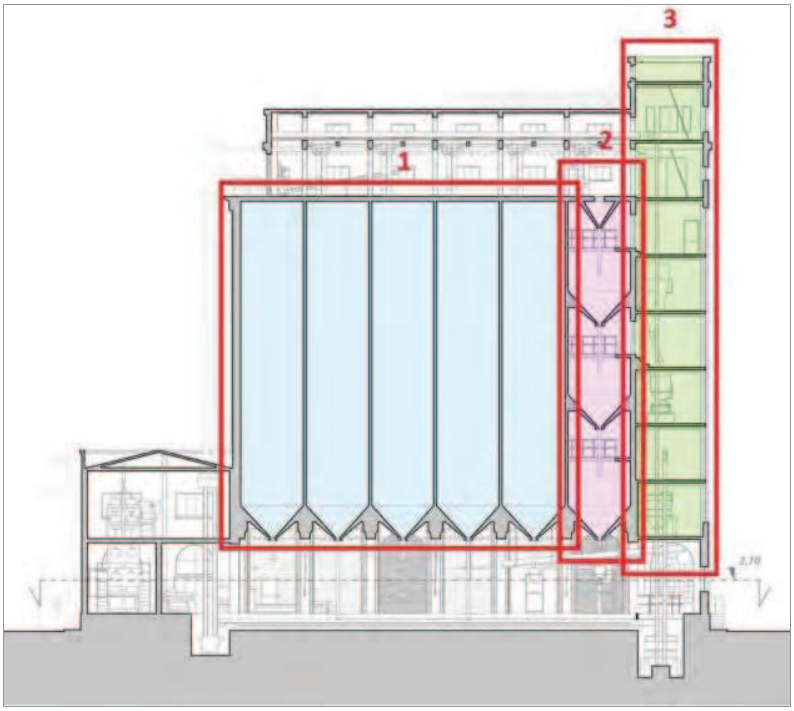

Figure 7 Longitudinal section of the silo

Legend:

(1) Vertical Cells
3.80 x 3.80 x 18.00 m;

(2) Vertical Cells
3.80 x 3.80 x 6.00 m;

(3) '*Torretta*'.

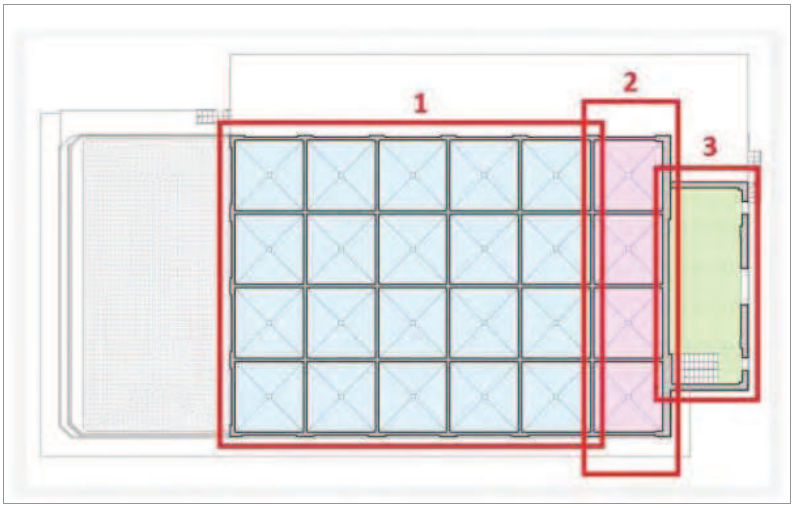

Figure 8 Plan view of the silo's cells

Legend:

(1) Vertical Cells
3.80 x 3.80 x 18.00 m;

(2) Vertical Cells
3.80 x 3.80 x 6.00 m;

(3) '*Torretta*'.

3.2 Decision on immediate actions

From the information collected so far, it is possible to evaluate the forces acting on the structural elements of the silo.

The next operations to perform in view of assessing the actual safety level, are:

- a survey of the current state of decay of the building and of the structural materials;
- the survey of the crack patterns;
- the so-called *simulated design*, aimed to reconstruct the most probable arrangements of the rebars in the different sections of the structural elements;
- the structural analysis based on the current static model and the state of materials.

4 DETAILED ASSESSMENT

4.1 Detailed documentary search and review

The fundamental design rules for r.c. structures in the 19th's were collected in some technical texts [14], [17], [18] and handbooks [20], in which it is also possible to find the characteristics of the most employed materials.

Loose materials which are stored in the silos apply pressure on the walls of the cells [14]. The values of the pressure could be calculated following the *theory of earth pressure*, which assumptions are met since we have homogeneous materials, but, in the case of the silos, the cross section is small in comparison to its height, so it is demonstrated that pressures are smaller than those calculated following the Rankine theory for earth pressure and they tend to a limit value below a certain depth.

Janssen [10] and Koenen [11] faced the study of the horizontal and vertical pressures in a silo; their results are still valid and the values of certain coefficients have been obtained from experiences.

Knowing the main dimensional parameters of the silo and the kind of material stored in it, it is possible to calculate the horizontal and vertical pressures, through which the stress patterns in structural elements and in the walls of the cells can be determined [17], [18].

4.2 Detailed visual inspection

The first step to investigate the actual state of the silo is a visual survey, that can be subdivided in three sub-steps: dimensional survey, materials survey and decay survey.

The dimensional survey (Fig. 9, 13, 17) has been carried out by means of the polygonal measurements, in order to minimize errors.

As a result, the main resistant elements have been identified, and their dimensions measured, so that it has been possible to understand the silo's static scheme:

- the ground floor works as a *pilotis* floor, composed by a set of pillars, with different cross sections, and beams;
- the cells, composed by a continuous system of r.c. walls;
- the drying gallery and the "torretta" are sustained by frames with pillars and beams.

All the different parts are connected to each other, to form a unique structure.

The building materials have been identified and indicated on a map by different colors (fig. 10, 14, 18). The structural elements and the walls are all made of reinforced concrete, covered with a thick layer of plaster.

The survey allowed to identify the main decay and deterioration phenomena (fig. 11, 15, 19); the results are summarized and classified in a specific table (table 1) and in a photo gallery (fig. 12, 16, 20). Globally, the building appears in a good state of maintenance .The phenomena

observed are those typical of ageing reinforced concrete structures, but are not related to instability or overstress, since no crack pattern has been observed.

It had been also possible to identify, in a pillar of the ground floor, a smooth longitudinal rebar, 30 mm in diameter, and a 16 mm diameter stirrup.

Some relevant examples of the survey are shown below: for each one, the geometrical and material data are represented on maps and a photo gallery showing the main decay phenomena.

Table 1 Degradation types and causes

CLASSES	DEGRADATION	MAIN CAUSES	TAG
A LOSS OF PLASTER	Total loss of plaster	Atmospheric agents Thermal and hygrometric variations Moisture action	A1
	Partial loss of plaster	Lack of maintenance Action of rising moisture	A2
B MOISTURE ACTION	Moisture action	Thermal and hygrometric variations Action of rising moisture	B
C PATINA	Biological patina	Wind and rain Action of rising moisture	C1
	Efflorescence	Water infiltration Salt crystallization	C2
	Stain	Thermal and hygrometric variations Moisture action	C3
D	Plaster reintegration with cement mortar or other materials	Anthropogenic causes	D
E	Lack of elements	Lack of maintenance Anthropogenic causes Action of rising moisture	E
F	Not Cross Cracks	Atmospheric agents Thermal and hygrometric variations Moisture action	F
G	Overgrown plants	Favorable hydrothermal and sunshine conditions	G
H	Differential degradation	Lack of maintenance Anthropogenic causes Action of rising moisture	H
I	Corrosion of steel rebars	Carbonation action Chlorides action	I

4.2.1 Ground Floor

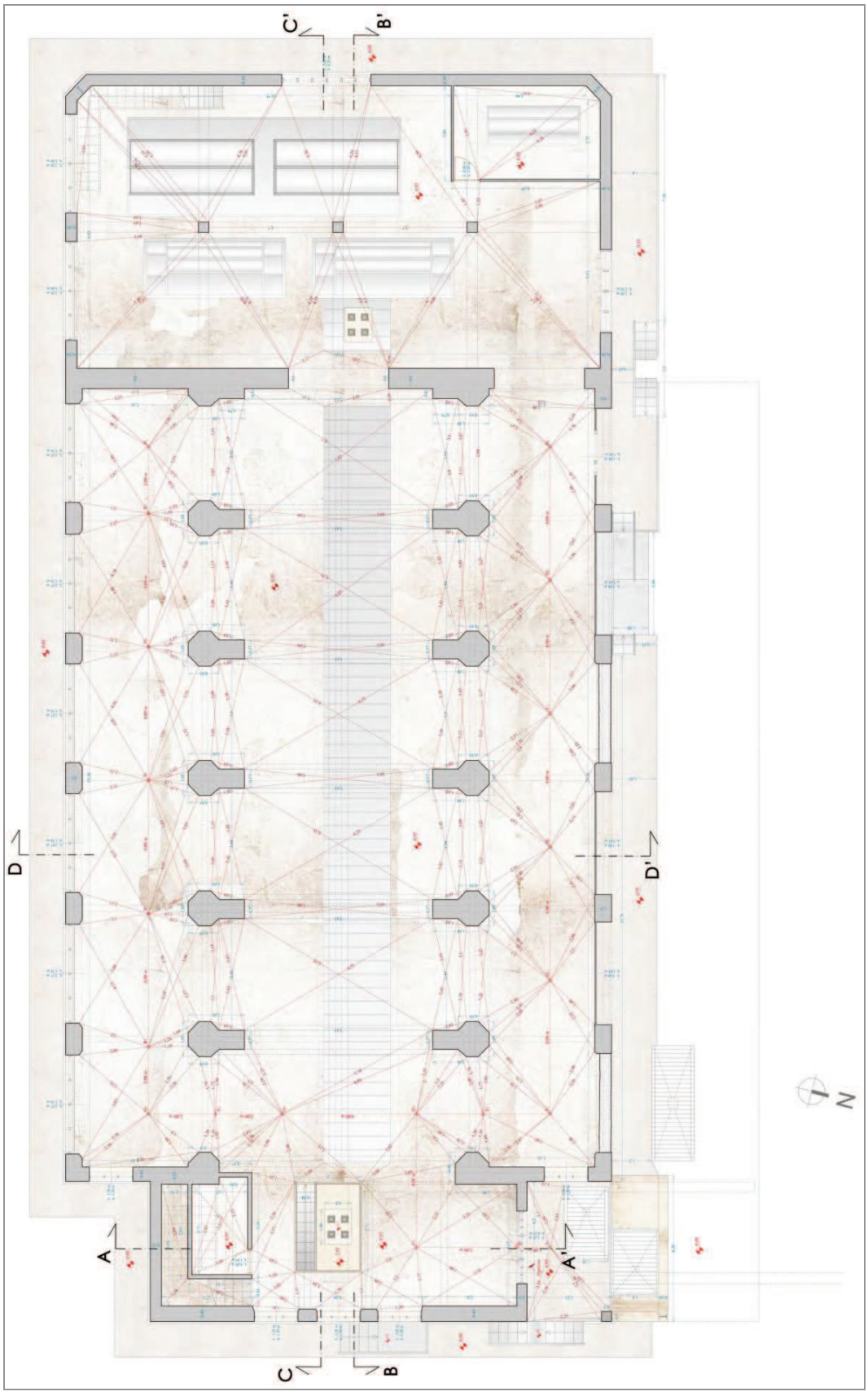

Figure 9 Example of dimensional survey: ground floor map

Figure 10 Example of the building materials survey: ground floor map

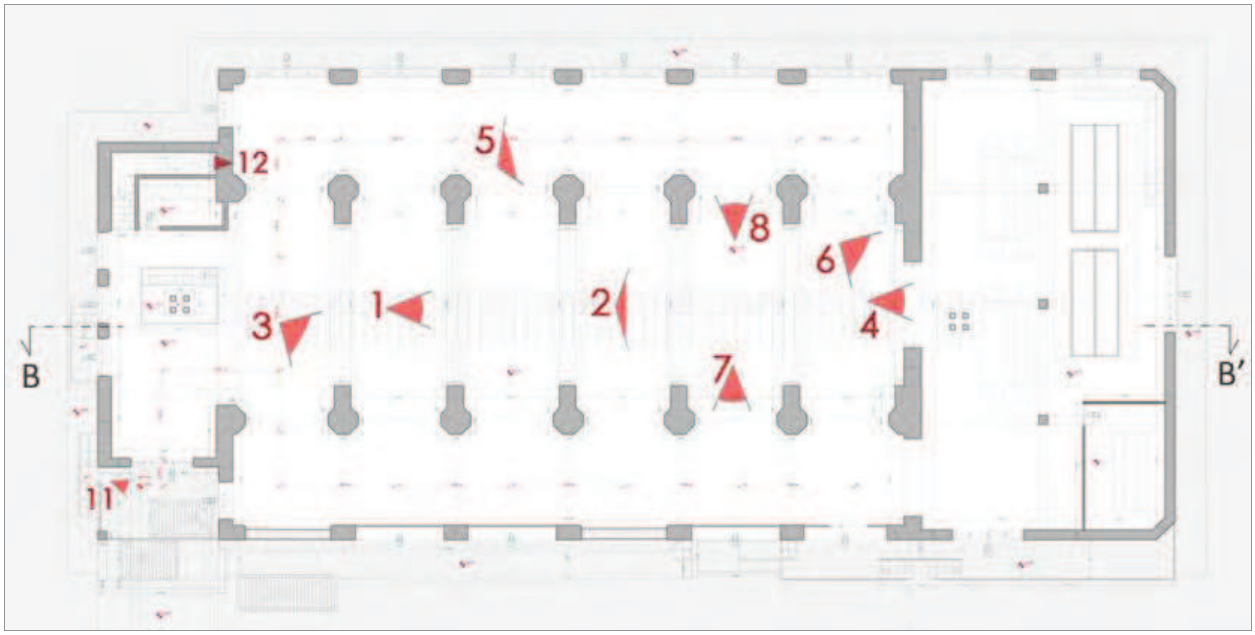

Figure 11 Example of the decay survey: ground floor map

Picture 1: Internal view of the ground floor: lack of cracks, presence of several patina

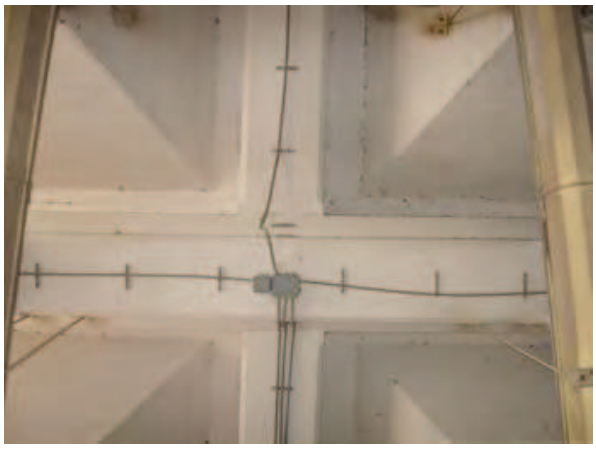

Picture 2: Detail of the beams-hoppers system: lack of cracks

Picture 3: Detail of the upper transport system of stored material. Presence of several patina and plaster reintegration with cement mortar on the attic

Picture 4: Detail of ground floor dusts and vertical transport system of stored materials

Picture 5: Detail of the beams, pillars and hoppers system: lack of cracks, presence of some patina

Picture 6: Detail of the work system of stored material. Presence of several patina and plaster reintegration with cement mortar on the attic

Figure 12 Photo gallery: ground floor (with reference to fig. 11)

Picture 7: Detail of the flooring. Presence of several patina and cracks

Picture 8: Detail of the flooring. Presence of several patina and relevant not cross cracks

Figure 12 (continuation) Photo gallery: ground floor (with reference to fig. 11)

4.2.2 Longitudinal Section BB'

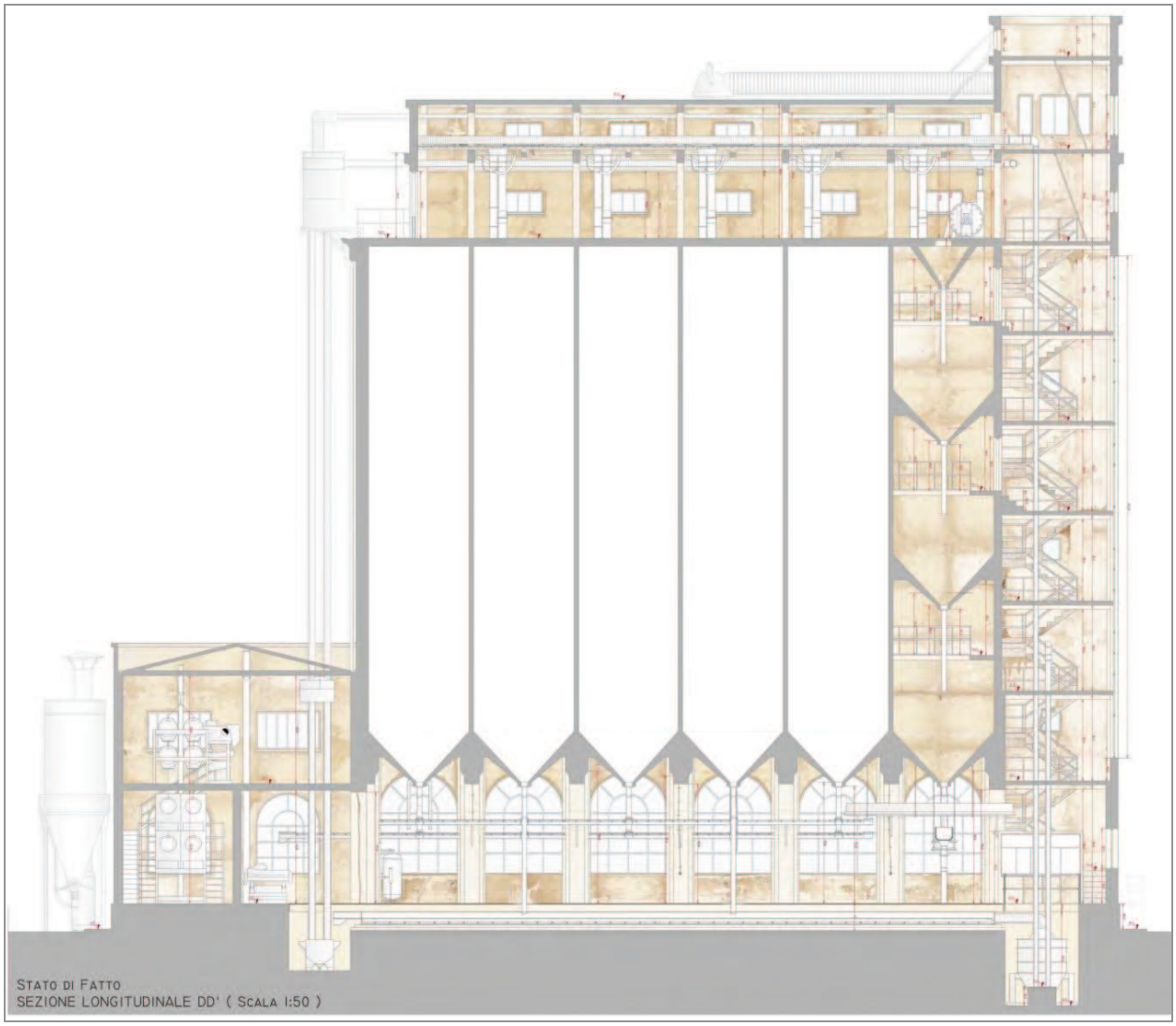

Figure 13 Example of dimensional survey: longitudinal section BB'

Figure 14 Example of building materials survey: longitudinal section BB'

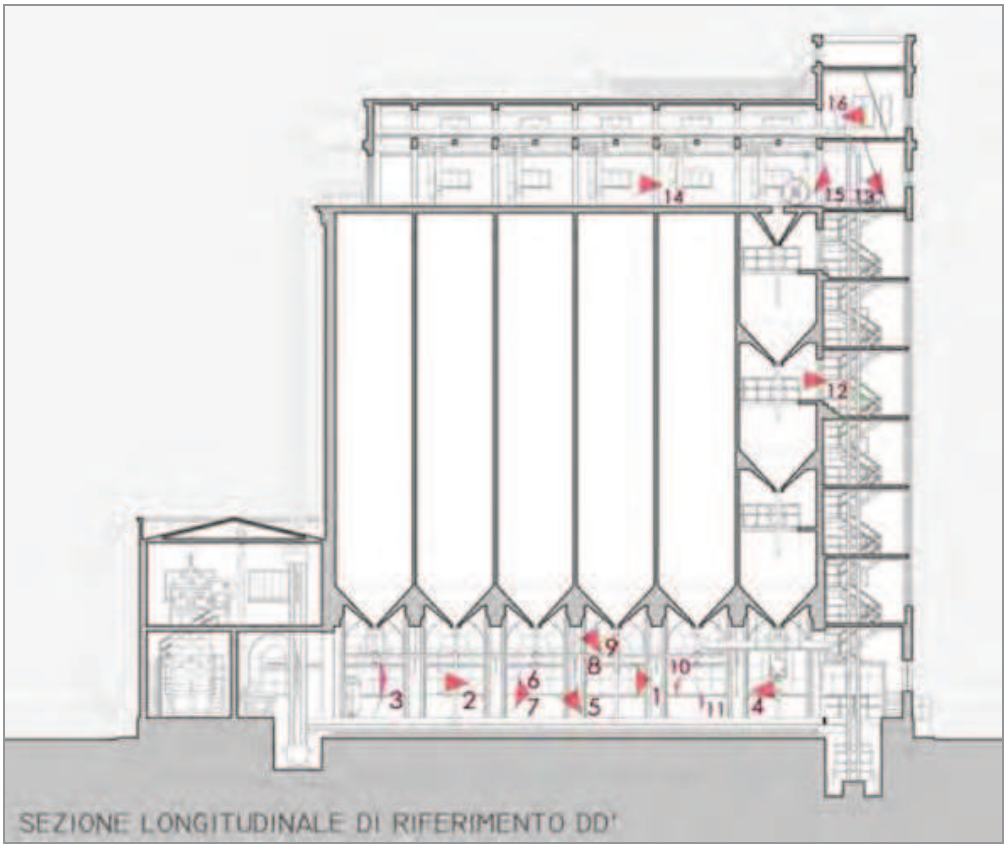

Figure 15 Example of decay survey: longitudinal section BB'

Picture 1: Internal view of the upper transport system: presence of several patina (Class D)

Picture 2: Detail of the arch, dust and caos

Picture 4: Detail of a window, dust and caos

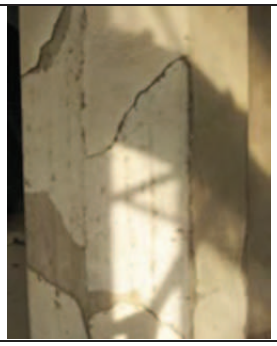

Picture 6: Detail of partial lack of plaster in the pillar (A1)

Picture 9: Detail of joint between pillar top and attic: presence of not cross crack and stain

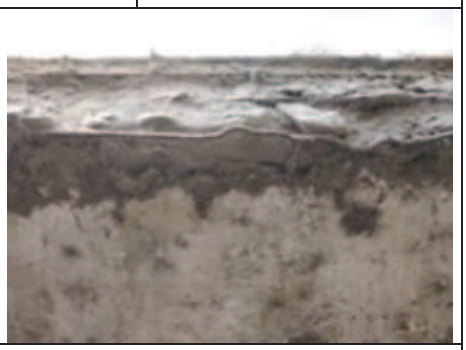

Picture 11: Detail of curtain under the window. Lack of concrete cover and presence of dust and several patina

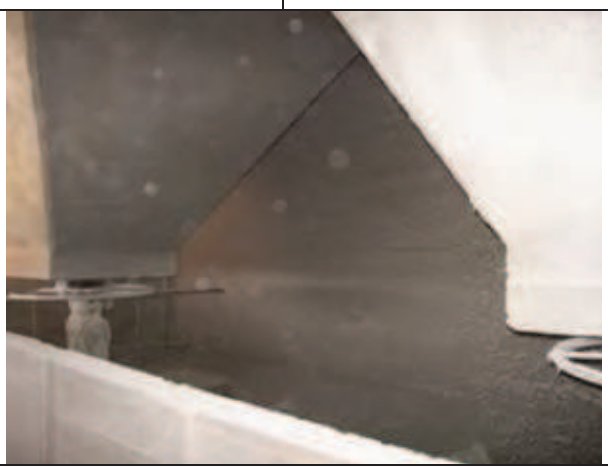

Picture 12: View of vertical cells interior. There is dust due to the silo which is still working

Picture 13: Detail of the hole in the upper flat roof. Presence of moisture and patina

Figure 16 Photo gallery: longitudinal section BB' (with reference to Fig. 15)

		
Picture 14: View of drining gallery. Presence of several patina and not cross cracks	**Picture 15: Detail of the transport system of stored materials in the drining gallery. Prsence of patina and not cross cracks**	**Picture 16: View of the window. Lack of concrete cover, presence of dust and several patina**

Figure 16 (continuation) Photo gallery: longitudinal section BB' (with reference to Fig. 15)

4.2.3 The main façade survey

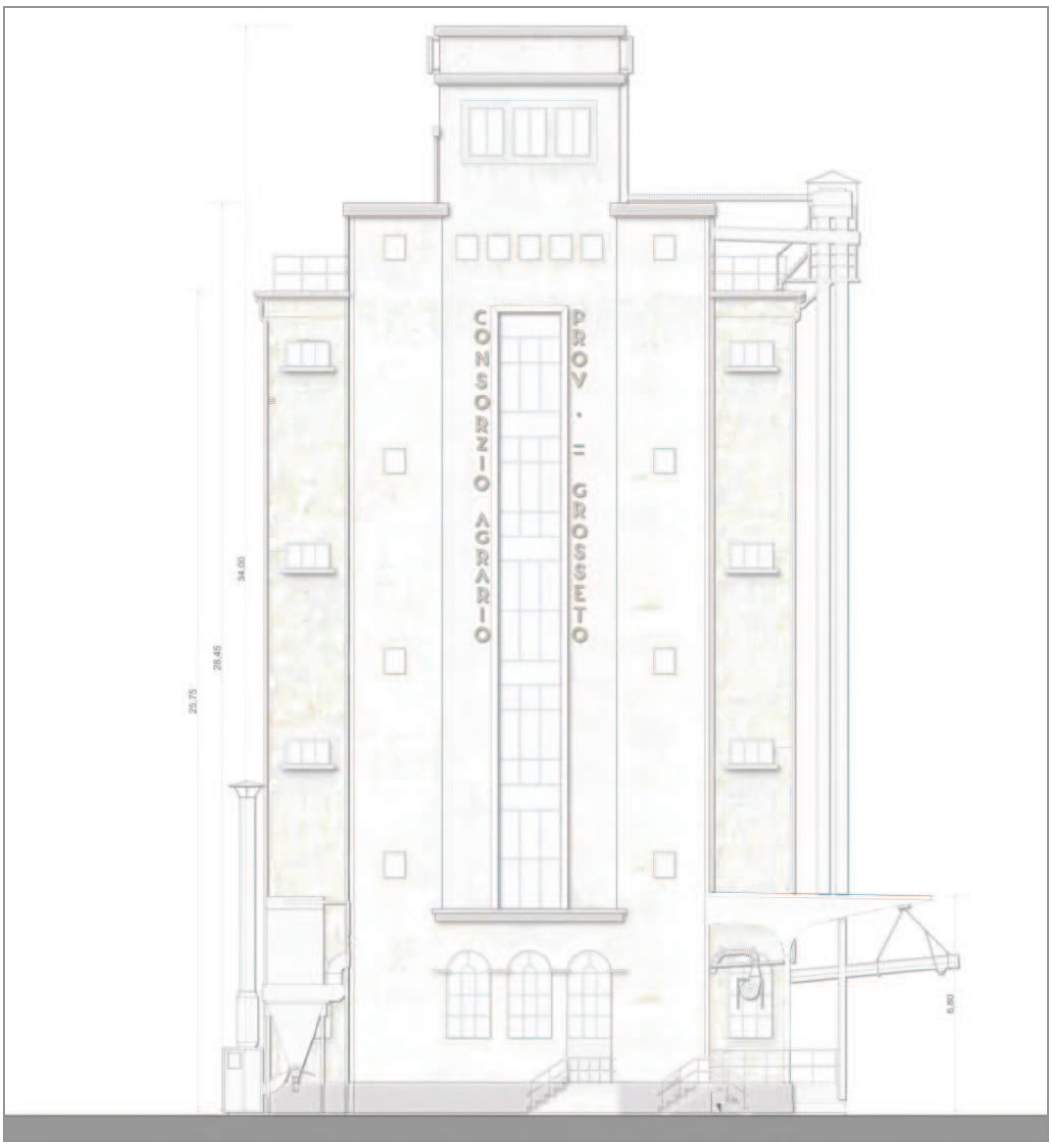

Figure 17 Example of dimensional survey: the main façade

Figure 18 Example of building materials survey: the main façade

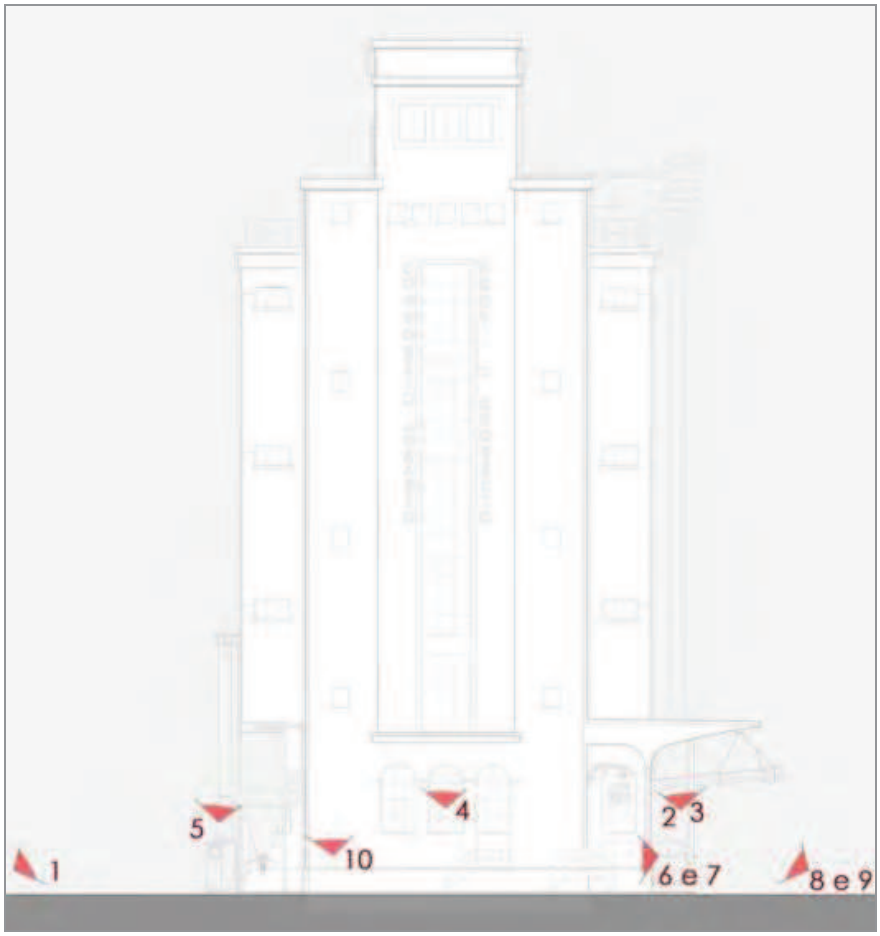

Figure 19 Example of decay survey: the main façade

Picture 1 (left): External view of the silo: presence of several patina (Class D)

Picture 2 (right): External view of the silo: presence of several patina (Class D)

Picture 6: Detail of the façade: presence of several patina, moisture and stain

Picture 9: Detail of the upper façade: presence of several patina, moisture and stain

Picture 11: Detail near the upper string course. Lack of concrete cover and presence of dust and several patina

Picture 12: Detail of the bottom façade: presence of several patina, moisture and stain

Picture 13: Detail of the hole to reach the upper flat roof. Presence of moisture and patina

Figure 20 Photo gallery: the main façade (with reference to Fig. 19)

As it is clear from the images above, the main degradation phenomena are constituted by patina (class C) on the internal, external and flat surfaces of the silo, probably due to the perishable stored materials which accelerate the biological attack, and even to negligence. Other decay phenomena frequently detected are not-cross cracks, that often have determined partial loss of plaster, and in some cases, deterioration of the concrete cover, and even the corrosion of steel rebars. In some structural elements the plaster was refurbished with cement mortar.

In conclusion, the decay phenomena analysis shows no symptom of activation of failure mechanisms: cracks are limited to the plaster and do not affect the r.c. element. All the phenomena are primarily caused by lack of maintenance during the years.

4.3 Structural analysis

The structural analyses has been performed with reference to the stability of the r.c. walls of the cells, taking into account the characteristics of materials, concrete and steel, accordingly to what found in the literature of the building time. So the probable quantity of reinforcing bars in the walls has been evaluated. Before proceeding to eventual interventions, in situ tests to determine the real quality of concrete and steel and the number and diameters of the rebars should be performed. The information obtained from the detailed analyses will be useful for limiting the extension and invasiveness of the tests.

4.3.1 Determination of actions

The main actions which affect the structure of the silo are induced by the materials stored in the cells: the pressure exerted by the stored materials can be evaluated following the *Janssen theory*, and the subsequent stresses accordingly to the *Ritter theory of plane frames*.

It is assumed that for a cell the following characteristics remain constant:

- A = area of the inner section of the cell;
- l =length of the inner perimeter of the cell;
- φ = angle of internal friction of the stored material (assumed incoherent);
- γ = specific weight of the material;
- δ = angle of friction between the material and the containing wall.

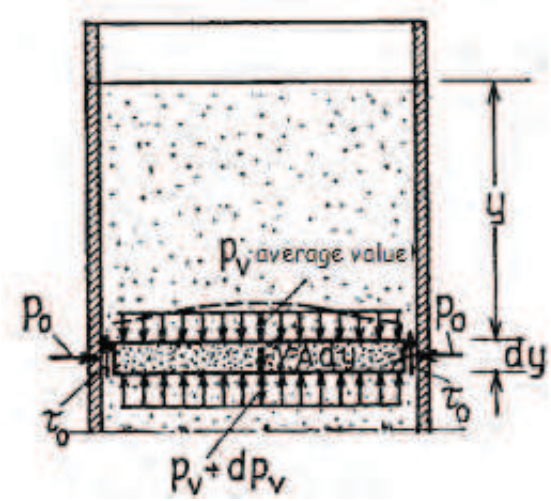

Figure 21a Horizontal and vertical pressures on a horizontal section of a cell, according to the Janssen theory

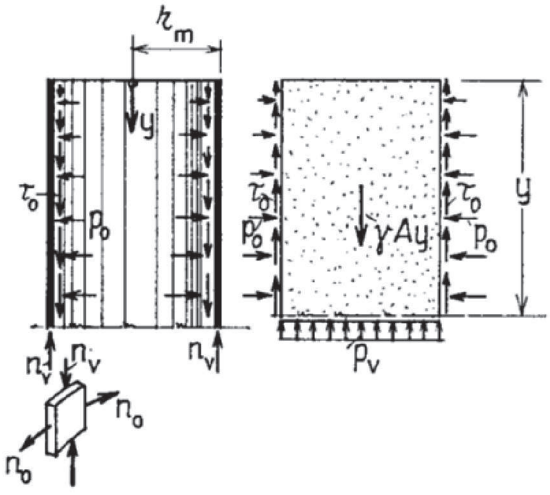

Figure 21b Pressures and actions in a general silo section

Janssen theory assumes that in a generic horizontal section of the cell the vertical pressure is uniformly distributed (Fig. 21a), so that the equilibrium equation in the vertical direction for a layer of material whose thickness is infinitesimal can be written:

$$-dp_v \cdot A - \tau_o l \cdot dy + \gamma A \cdot dy = 0 \tag{1}$$

where:

- p_v : vertical pressure;
- p_o : horizontal pressure;
- τ_o : shear stress on the boundary.

Stated that:

$$\frac{p_o}{p_v} = \lambda \qquad \frac{\tau_o}{p_o} = tg\delta = f \qquad \frac{\tau_o}{p_v} = \lambda \cdot f \tag{2}$$

equation (1) can be rewritten:

$$\frac{dp_v}{dy} + \frac{\lambda \cdot f \cdot l}{A} \cdot p_v - \gamma = 0 \tag{3}$$

Supposing that λ, f, γ maintain constant through y, and setting:

the characteristic depth $y_0 = \frac{A}{\lambda \cdot f \cdot l}$ and $1 - e^{-y/y_0} = \psi(y)$ (4)

the solution of (3) is:

$$p_v = \gamma \cdot y_0 \cdot \psi(y) \tag{5}$$

$$p_o = p_v \cdot \lambda = \gamma \cdot y_0 \cdot \lambda \cdot \psi(y) = \frac{\gamma \cdot A}{f \cdot l} \cdot \psi(y) \tag{6}$$

Experimental studies have confirmed that λ and f are practically constant with the depth, y, and that the pressure p_v is almost uniform in each horizontal section. On the other hand, the experiences show that the values of the pressures, for a given filling level, are sensibly different when the material is at rest from when it is moving (unloading operation); specifically, p_v is greater at rest while p_o is greater at the unloading.

For the p_v it is important to know not only the maximum value but also the minimum, which corresponds to the maximum load hanging on the wall due to the friction (Fig. 21b). The vertical normal stress, n_v, in the wall is equal to the difference between the weight of the material above the generic height y and the reaction $p_v A$ of the material below (l_m is the length of the medium line between the outer and the inner contour):

$$n_{v\max} = (\gamma \cdot y - p_{v,\min}) \cdot A : l_m \tag{7}$$

In order to evaluate the level of pressure on the silo's walls, it's important to take into account the behaviour of the material stored inside. In particular, the situation changes according to the characteristics of material (granular or powdered material) and to the two different conditions, static or dynamic, when the outfalls are close or open.

Indeed, the coefficients λ, f, and δ depend on the characteristics of material (angle of friction), on the roughness of the walls and on the condition (static or dynamic). In Annex A the values adopted for the case study, a silo containing cereals, are given, as derived from the manuals of the time [14].

The trend of the pressures along the height of the cell is defined by the equations (5) and (6); using the specific coefficients for the dynamic and static condition we have two different functions for each case (horizontal pressure and vertical pressure).

In the dynamic condition, the horizontal pressures, along the height of the cell, are higher than in the static condition; but in the vicinity of the outlet hole the pressure is smaller than that resulting from equation (6). To take account of that, it is correct to assume for the dynamic pressure:

- the value of the static pressure at the bottom of the cell
- the value of the dynamic pressure at a height h_f from the bottom
- and a linear variation between the two values from the bottom to h_f.

The height h_f is the lower of the following two values:

$$h_f' = 2d \qquad h_f'' = \frac{H}{3} \tag{8, 9}$$

where:

d = is the diameter of the maximum circle inscribed in the cell;
H = is the total height of the cell.

In figs. 22, 23, the diagrams of p_v and p_o for the single cell of the case study, both in the static and in the dynamic condition. In Annex A the evaluation of the pressures is illustrated.

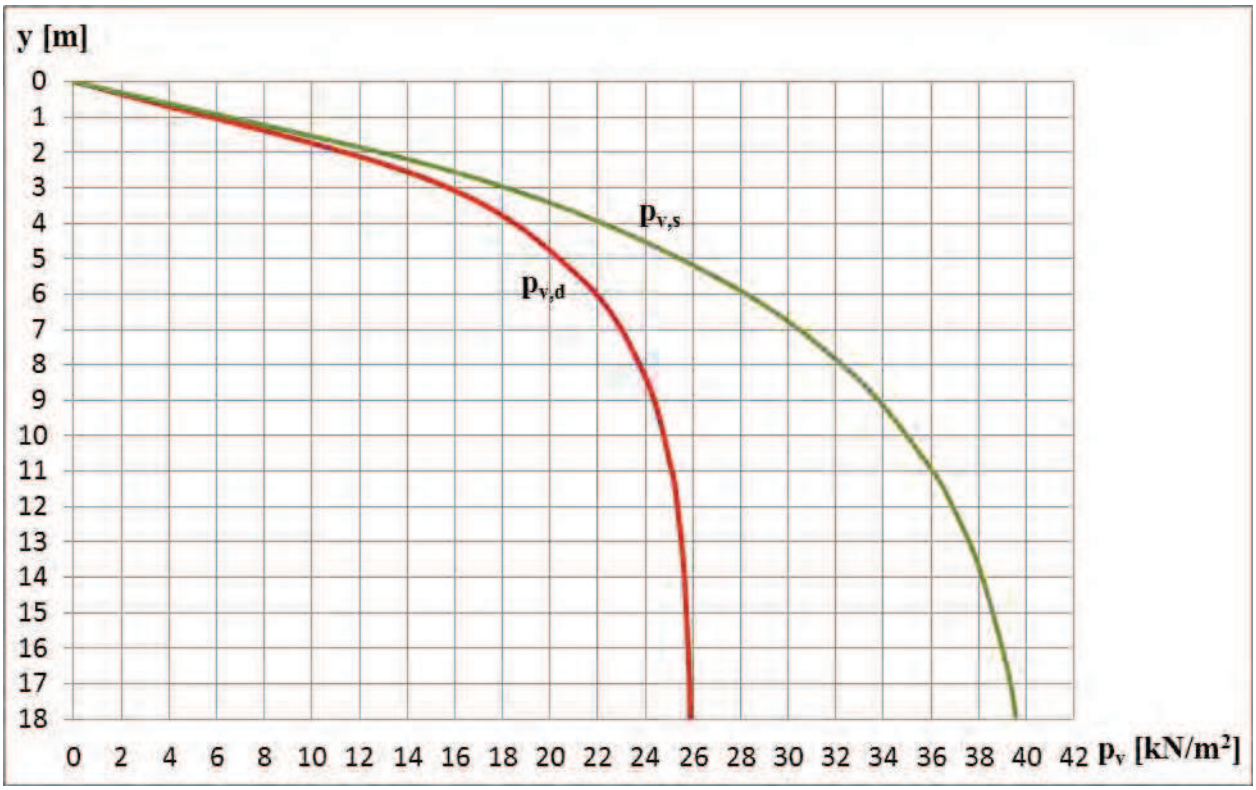

Figure 22 Actual vertical pressure diagram along the height of the cell

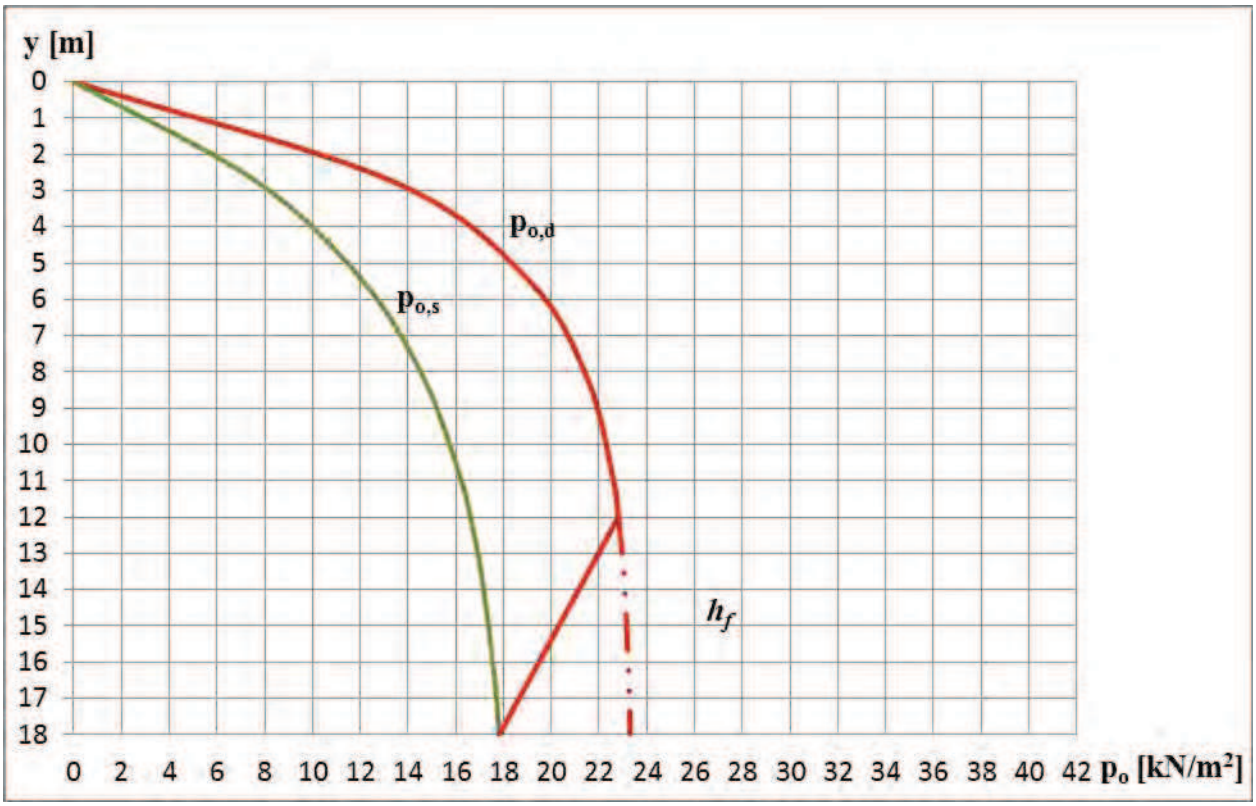

Figure 23 Actual horizontal pressure diagram along the height of the cell

4.3.2 Stresses evaluation

In a group of cells, all full, only the external walls of the perimeter are subjected to bending, while the internal ones are subjected only to tension. The loading conditions which generate the maximum bending moments are:

– chessboard load (fig. 24) to which correspond the maximum moments at the centreline;
– load in the cells of a row (fig. 25) which gives the maximum negative moments.

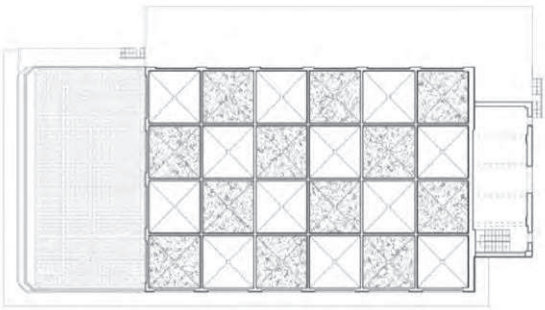

Fig. 24: Chessboard load.

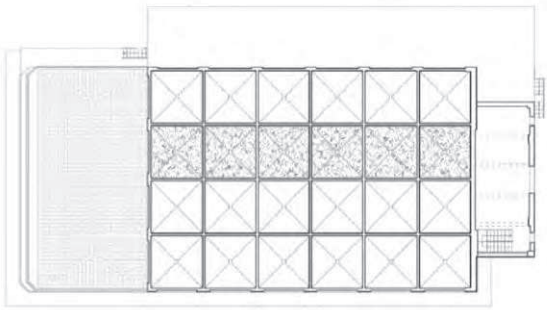

Fig. 25: Load in the cells of a row.

In a finite group of cells, the stresses may be evaluated considering a horizontal slice of the cells with unitary height, as a frame in the horizontal plane.

Given that no modern structural modelling was available at the time of building, the values of the bending moment are calculated following the Ritter theory. For the loading condition of fig. 24, the loaded cell is considered isolated from the others and it is calculated as a close frame loaded by the internal pressure, orthogonal to the walls (fig. 26).

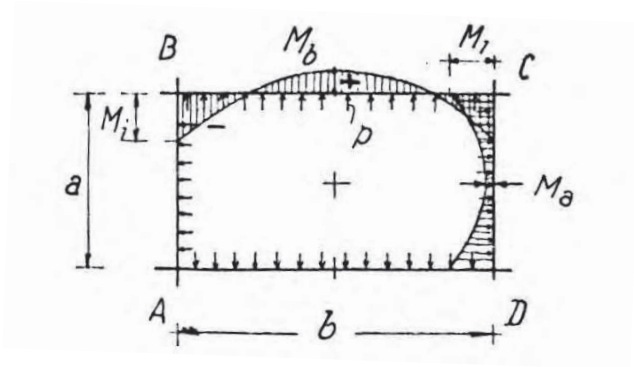

Figure 26 Cell calculated as a close frame loaded by the internal pressure, orthogonal to the walls

For square cells (side *a*) of constant thickness, the values of the bending moments at the joints, M_j, and in the centreline, M_m, are:

$$M_j = -\frac{p_o}{12} \cdot a^2 \qquad M_m = \frac{p_o}{24} \cdot a^2 \qquad (10, 11)$$

The walls of an internal cell are subjected not only to flexure, but also to tension. In the chessboard load condition, it occurs the maximum bending moment in the walls, but not the maximum tension. In this case the tension is:

$$N = p_o \cdot \frac{a}{2} \qquad (12)$$

while, if the cell adjacent on the side b (see fig. 25) is full, the tension is:

$$N = p_o \cdot a \qquad (13)$$

When all the cells are full, in the internal walls acts only the maximum tension and there is no bending moment.

With chessboard load, in the outside walls of the external cells both the tension and the bending moment are maximum.

4.4 Determination of properties of the structure.

Once the maximum stresses have been calculated as described above, the evaluation of the amount of rebars is done accordingly to the Italian standards valid at the time (R.D.L. 07/06/1928 n. 1431) and to proven texts of that period [17], [18].

The verification method is the allowable strength; the modular ratio is taken m=10 and the rebars are supposed to be symmetrically distributed.

The calculations are shown in Annex A.

5 CONCLUSIONS

The assessment of a historical silo has been discussed, with particular emphasis on simulation of original design, carried out on the basis of the relevant literature and codes available when the silo was built, demonstrating that this procedure is a valuable help in understanding the structural scheme and the detailing of the building.

REFERENCES

[1] ISO 13822 (2001) Basis for design of structures - Assessment of existing structures. ISO, Geneva, Switzerland.

[2] EN1992 – 1-1, Eurocode 2 – Design of concrete structures. Part 1-1: General rules and rules for buildings, CEN, Brussels 2006.

[3] Chapperon R., Silo e magazzini per ammassi granari., Istituto delle edizioni accademiche, Udine, 1936.

[4] Crispolti E., Mazzanti A., Quattrocchi L., Arte in Maremma nella prima metà del Novecento, Silvana Editore, Grosseto 2005.

[5] Croce P., Holický M. eds. (2013) Operational methods for the assessment of existing structures.
http://www.leonardo.cvut.cz/download/march2014/Operational_Methods_for_the_Assessment_of_Existing_Structures.pdf

[6] Dalla Negra R., Nuzzo M., L'architetto restaura: guida al laboratorio di restauro architettonico, Spring Edizioni, Caserta 2008.

[7] Diamantidis D., Holický M. eds. (2012) Innovative methods for the assessment of existing structures. CTU in Prague, Klokner Institute, Prague.
http://www.leonardo.cvut.cz/download/Innovative_Methods_for_the Assessment_of_Existing_Structures.pdf

[8] Docci M., Maestri D., Manuale di rilevamento architettonico e urbano, Laterza, Bari 2009.

[9] Ientile R., Tempestività di intervento e autenticità, in La conservazione del calcestruzzo armato nell'architettura moderna e contemporanea: monumenti a confronto, in Quaderni di Ananke n.2, pag.51, Milano 2010.

[10] Janssen, H.A., Versuche uber Getreidedruck in Silozellen, VDI Zeitschrift, 1895.

[11] Koenen, Berechnung des Seiten u. Bodendruckes in Silozellen, Centralblatt der Bauverwaltung, 1896.

[12] Mariani F., Depositi, magazzini e sili, Bazzi editore, Milano, 1940.

[13] Nelvi R., Signorelli B., Avvento ed evoluzione del calcestruzzo armato in Italia: il sistema Hennebique, AITEC, Milano 1990.

[14] Pozzati P., Teoria e tecnica delle strutture. Volume I. Preliminari e fondamenti. Ed. UTET, Torino, 1972.

[15] Readelli E., Come intervenire senza sostituire, in La conservazione del calcestruzzo armato nell'architettura moderna e contemporanea: monumenti a confronto, in Quaderni di Ananke n.2, pag.70, Milano 2010.

[16] Ritter, Armiert. Beton, 1913.

[17] Santarella L., Il cemento armato. Volume II. Le applicazioni alle costruzioni civili ed industriali., Ed. n° 14, 1975.

[18] Santarella L., Il cemento armato. Volume I. La tecnica e la statica., Ed. n° 19, 1975.

[19] Zevi B., Storia dell'architettura Moderna, Torino 1950.

[20] Manuale dell'ingegnere, Colombo G., 80a Edizione, Hoepli, 1971.

CHAPTER 4 - ANNEX A
CALCULATION OF PRESSURES AND STRESSES IN THE SILO

A.1 DATA

h	=	18,00	m	(maximum height of vertical cells)
a	=	3,80	m	(length of the inner side of a cell)
s	=	0,17	m	(thickness of the walls of the cell)
A	=	14,44	m^2	(area of the inner section of a cell)
l	=	15,20	m^2	(length of the inner perimeter of a cell)
φ	=	30°		(friction angle of the stored material, wheat)
γ	=	8,00	kN/m^3	(specific weight of the material, wheat)

All these characteristics are supposed to be constant.

As mentioned in §4.3.1, the coefficients λ, f, and δ depend on the characteristics of the stored material, on the roughness of the walls and on the condition, static or dynamic, i.e. material at rest or unloading.

For the two conditions, the values of such coefficients as derived from the manuals of the time [14], are shown in Table A.1, where:

δ_s is the friction angle between the stored material and the wall in the static condition
δ_d is the friction angle between the stored material and the wall in the dynamic condition
$f_s = tg\delta_s$ is the friction coefficient in the static condition
$f_d = tg\delta_d$ is the friction coefficient in the dynamic condition

Table A.1 Values of coefficients λ, f, and δ for a silo containing wheat.

	STATIC CONDITION			DYNAMIC CONDITION		
φ	δ_s	f_s	λ_s	δ_d	f_d	λ_d
30°	0,75 φ	0,41	0,45	0,60 φ	0,32	0,9

A.2 EVALUATION OF THE PRESSURES

a) **Evaluation of the *Characteristic Depth***

a.1) Evaluation of the *Characteristic Depth*, $y_{0,s}$ in the static regime:

$$y_{0,s} = \frac{A}{\lambda_s \cdot f_s \cdot l} = \frac{14,44}{0,45 \cdot 0,41 \cdot 15,20} = 5,10\text{m} \qquad \text{(A1)}$$

a.2) Evaluation of the *Characteristic Depth*, $y_{0,d}$, in the dynamic regime (unloading phase):

$$y_{0,d} = \frac{A}{\lambda_d \cdot f_d \cdot l} = \frac{14,44}{0,90 \cdot 0,32 \cdot 15.20} = 3,25\,\text{m} \qquad \text{(A2)}$$

b) **Evaluation of the *Horizontal Pressures***

b.1) The *Minimum Horizontal Pressure*, $p_o(y)$, occurs when the material is at rest and it depends on the characteristic depth in static regime, $y_{0,s}$. It can be derived evaluating p_o, which depends on y, as:

$$p_{o,s} = \frac{\gamma \cdot A}{f_s \cdot l} \cdot \psi(y_i) = \frac{8{,}00 \cdot 14{,}44}{0{,}41 \cdot 15{,}20} \cdot \psi(y_i) = 18{,}35 \frac{\text{kN}}{\text{m}^2} \cdot \psi(y_i) \tag{A3}$$

where:

$$\psi(y) = 1 - e^{\frac{-y}{y_0}} \tag{A4}$$

The distance h_f is:

$$h_f = \frac{H}{3} = \frac{18{,}00}{3} = 6{,}00\text{m} \tag{A5}$$

b.2) The *Maximum Horizontal Pressure*, $p_o(y)$, occurs during the unloading phase, therefore the *Horizontal Pressure Diagram* is calculated in dynamic condition and it depends on the characteristic depth in dynamic regime, $y_{0,d}$. It can be derived evaluating p_o, which depends on y, as:

$$p_{o,d} = \frac{\gamma \cdot A}{f_d \cdot l} \cdot \psi(y_i) = \frac{8{,}00 \cdot 14{,}44}{0{,}32 \cdot 15{,}20} \cdot \psi(y_i) = 23{,}39 \frac{\text{kN}}{\text{m}^2} \cdot \psi(y_i) \tag{A6}$$

where:

$$\psi(y) = 1 - e^{\frac{-y}{y_0}} \tag{A7}$$

Using the equations (A1) through (A7) and the Table A.1, the values of the horizontal pressure along the height of the cell are evaluated (see Fig. 23 in §4.3.1).

Table A.2 Horizontal pressures

	Section 1	**Section 2**	**Section 3**	**Section 4**	**Section 5**	**Section 6**	**Section 7**	**Section 8**	**Section 9**
y_i **(m)**	0.00	2.74	5.48	8.22	10.96	12.00	13.71	16.45	18.00
ψ_s	0.00	0.42	0.66	0.80	0.88	0.91	0.93	0.96	0.97
$p_{o,s}$ **(kN/m²)**	0.00	7.63	12.09	14.69	16.21	16.61	17.10	17.62	17.81
$p_{o,d}$* **(kN/m²)**	0.00	13.33	19.06	21.53	22.59	22.81	21.38*	9.10*	7.81*

* reduced values from a height of 6 metres from the bottom.

c) **Evaluation of the *Vertical Pressures***

c.1) The *Maximum Vertical Pressure*, $p_v(y)$, occurs when the material is at rest and it depends on the characteristic depth in the static regime, $y_{0,s}$. It can be derived evaluating p_v, which depends on y, as:

$$p_{v,s} = \gamma \cdot y_{0,S} \cdot \psi(y_i) = 8{,}00 \cdot 5{,}10 \cdot \psi(y_i) = 40{,}80 \frac{\text{kN}}{\text{m}^2} \cdot \psi(y_i) \tag{A8}$$

c.2) The *Minimum Vertical Pressure*, $p_v(y)$, occurs when the material is at rest and it depends on the characteristic depth in dynamic regime, $y_{0,d}$. It can be derived evaluating p_o, which depends on y, as:

$$p_{v,d} = \gamma \cdot y_{0,d} \cdot \psi(y_i) = 8{,}00 \cdot 3{,}25 \cdot \psi(y_i) = 26{,}00 \frac{\text{kN}}{\text{m}^2} \cdot \psi(y_i) \tag{A9}$$

Using the equations (A1), (A2), (A8), (A9) and the Table A.1, the values of the vertical pressure along the height of the cell are evaluated (see Fig. 22 in §4.3.1).

Table A.3 Vertical pressures

	Section 1	Section 2	Section 3	Section 4	Section 5	Section 6	Section 7	Section 8	Section 9
y_i (m)	0.00	2.74	5.48	8.22	10.96	12.00	13.71	16.45	18.00
ψ_d	0.00	0.57	0.81	0.92	0.97	0.98	0.99	0.99	1.00
$p_{v,s}$ (kN/m^2)	0.00	16.96	26.86	32.65	36.03	36.90	38.01	39.16	39.58
$p_{v,d}$ (kN/m^2)	0.00	14.81	21.18	23.92	25.10	25.34	25.61	25.83	25.89

d) Evaluation of the maximum vertical normal stress, n_v

Using the equation (7) §4.3.1 the values of the maximum vertical normal stress are calculated. They depend on the dynamic condition and are connected to the minimum values of the vertical pressure, $p_{v,d}$.

Table A.4 Vertical normal stresses

	Section 1	Section 2	Section 3	Section 4	Section 5	Section 6	Section 7	Section 8	Section 9
y_i (m)	0.00	2.74	5.48	8.22	10.96	12.00	13.71	16.45	18.00
ψ_d	0.00	0.57	0.81	0.92	0.97	0.98	0.99	0.99	1.00
$p_{v,d}$ (kN/m^2)	0.00	14.81	21.18	23.92	25.10	25.34	25.61	25.83	25.89
$n_{v,max}$ (kN/m)	0.00	6.76	21.53	39.75	59.45	67.12	79.87	100.49	112.21

A.3 EVALUATION OF STRESSES

The walls of the cells, being subjected to bending moment in both directions, are reinforced with two symmetrical series of horizontal rebars disposed in the vicinity of the surfaces, according to the diagram of pressures which increase from the top to the bottom. Usually the diameter of the horizontal rebars remains constant and the mutual distance in the vertical direction varies. Usually the reinforcing bars are maintained constant for the whole perimeter of the wall, therefore the sections where the stress is highest are considered. Indeed the sections to consider are those in the vicinity of the joints subject to the maximum bending moment, according to equation (10) §4.3.2, for the horizontal pressures in dynamic regime, $p_{o,d}$.

The stresses are evaluated for a slice high 100 cm of the internal walls or the external walls, and for the two situations: chessboard load and load in the cells of a row.

a) Internal walls

a.1) chessboard load:

$$M_1 = \frac{p_{o,d}}{12} \cdot a^2 \qquad N_1 = \frac{p_{o,d} \cdot a}{2} \qquad \text{(A10, A11)}$$

a.2) load in the cells of a row:

$$M_2 = 0 \qquad N_2 = p_{0,d} \cdot a \qquad \text{(A12, A13)}$$

b) External walls

b.1) chessboard load:

$$M_1 = \frac{p_{o,d}}{12} \cdot a^2 \qquad N_1 = \frac{p_{o,d} \cdot a}{2} \qquad \text{(A14, A15)}$$

For the design of rectangular sections in bending and axial force, following the verification method of the allowable strength which was in use at the time of the construction, it is possible to use tables which allow, once set a percentage of reinforcement, μ, to obtain coefficients to be used in the calculation of the stresses, σ_c and σ_s. Such coefficients, η_1, η_2, depend on the percentage of reinforcement, μ, on the modular ratio, m, and on the ratio β between the eccentricity, e, and the thickness of the section; also, there are different tables to be used in the case of simple or symmetrical reinforcement, and in the case of bending+compression or bending+tension.

For the case study, we have set:

- symmetric rebars
- $\mu = 2\%$;
- m=10.

Both for internal and external walls, in the chessboard load condition, the eccentricity, e, in the various sections is constant:

$$e = \frac{M}{N} = \frac{a}{6} = 0{,}63\text{m} \qquad \text{(A16)}$$

The corresponding coefficient β is:

$$\beta = \frac{e}{s} = 3{,}73 \qquad \text{(A17)}$$

Once defined the values of β and μ, it is possible to find, through Table A.5 (derived from [18]), the coefficients, η_1 and η_2, for the evaluation of the concrete and steel stresses, σ_c and σ_s.

$$\sigma_c = \frac{2 \cdot N}{s \cdot a} \cdot \eta_1 \qquad \sigma_s = \sigma_c \cdot \eta_2 \qquad \text{(A18, A19)}$$

The values of the stresses for the case study are shown in tables A.6 and A.7.

Table A.5 Coefficients for the calculation of stress in r.c. sections (derived from [18])

Tensoflessione - **Armatura simmetrica** $F_f = F'_f$.

$2\,F_f = \mu\,a\,b; \quad m = 10$

α	$\mu = 0{,}010$		$\mu = 0{,}015$		$\mu = 0{,}020$		η_2	η_3
	β	η_1	β	η_1	β	η_1		
0,290					∞	∞	22,66	8,17
0,280					11,654	29,17	23,82	8,11
0,270					5,753	14,14	25,06	8,04
0,265			∞	∞			25,74	8,00
0,260					3,801	9,15	26,42	7,96
0,255			10,270	30,11			27,14	7,92
0,250			6,883	20,00	2,828	6,67	27,88	7,88
0,240			4,127	11,76	2,246	5,17	29,45	7,79
0,232	∞	∞					30,82	7,72
0,230			2,932	8,19	1,858	4,17	31,17	7,70
0,220	7,980	28,95	2,266	6,18	1,583	3,46	33,05	7,59
0,210	4,242	15,11	1,841	4,90	1,376	2,92	35,10	7,48
0,200	2,867	10,00	1,547	4,00	1,217	2,50	37,35	7,35
0,180	1,717	5,70	1,168	2,83	0,986	1,88	42,61	7,06
0,160	1,213	3,77	0,935	2,09	0,828	1,45	49,19	6,69
0,140	0,933	2,67	0,780	1,58	0,715	1,13	57,64	6,21
0,120	0,757	1,95	0,669	1,20	0,630	0,87	68,92	5,58
0,100	0,638	1,43	0,588	0,91	0,564	0,67	84,70	4,70
0,075	0,538	0,95	0,514	0,62	0,503	0,46	116,27	2,93
0,050	0,471	0,57	0,462	0,38	0,458	0,28	179,40	−0,60
0,000	0,400	0,00	0,400	0,00	0,400	0,00	∞	−∞

Table A.6 Values of stresses in the chessboard load condition

	Section 1	Section 2	Section 3	Section 4	Section 5	Section 6	Section 7	Section 8	Section 9
y_i (m)	0.00	2.74	5.48	8.22	10.96	12.00	13.71	16.45	18.00
$p_{o,d}$ (kN/m^2)	0.00	13.33	19.06	21.53	22.59	22.81	21.38	9.10	7.81
M_1 (kN*m)	0.00	16.04	22.94	25.90	27.18	27.45	25.73	22.99	21.43
N_1 (kN)	0.00	25.32	36.22	40.90	42.92	43.34	40.63	36.29	33.84
η_1	8.96	8.96	8.96	8.96	8.96	8.96	8.96	8.96	8.96
η_2	26.53	26.53	26.53	26.53	26.53	26.53	26.53	26.53	26.53
σ_{c1} (N/mm^2)	0.00	2.67	3.82	4.31	4.52	4.57	4.28	3.82	3.57
σ_{s1} (N/mm^2)	0.00	70.80	101.26	114.37	120.01	121.17	113.61	101.48	94.63

Table A.7 Values of stresses in the situation of load in the cells of a row

	Section 1	Section 2	Section 3	Section 4	Section 5	Section 6	Section 7	Section 8	Section 9
y_i (m)	0.00	2.74	5.48	8.22	10.96	12.00	13.71	16.45	18.00
$p_{o,d}$ (kN/m^2)	0.00	13.33	19.06	21.53	22.59	22.81	21.38	9.10	7.81
M_2 (kN*m)	0.00	0.00	0.00	0.00	0.00	0.00	0.00	0.00	0.00
N_2 (kN)	0.00	50.64	72.43	81.81	85.84	86.67	81.26	72.59	67.68
σs_2 (N/mm^2)	0.00	14.89	21.30	24.06	25.25	25.49	23.90	21.35	19.91